Available online at www.sciencedirect.com

SciVerse ScienceDirect

Ceramics International 38 (2012) 3963–3967

CERAMICS INTERNATIONAL

www.elsevier.com/locate/ceramint

Domain structures in hot-press sintered $SrBi_2Ta_{1.6}Nb_{0.4}O_9$ and $SrBi_2Ta_2O_9$ ferroelectric ceramics

Wen Wang *, Jiancun Rao *, Hua Ke, Xianghe Meng, Dechang Jia, Yu Zhou

Institute for Advanced Ceramics, Department of Materials Science, Harbin Institute of Technology, Harbin 150001, PR China

Received 9 December 2011; received in revised form 18 January 2012; accepted 20 January 2012
Available online 27 January 2012

Abstract

$SrBi_2Ta_{1.6}Nb_{0.4}O_9$ (SBTN) and $SrBi_2Ta_2O_9$ (SBT) ceramics with typical bismuth layered perovskite structure were synthesized by hot-press sintering at 1000 °C for 2 h. The maximum relative density of as-sintered SBTN and SBT materials is 98.97%. The domain structure of SBTN and SBT was systemically characterized by means of TEM and HRTEM. The 90° domain walls were identified by the 90° rotation relationship of the electron diffraction pattern along the [0 0 1] zone axis. Irregular shaped and highly curved 180° domain wall were also observed in SBTN ceramics. The traditional α-fringes can be found in SBT, which are the evidence of large strains in hot-press sintering ceramics. Rod-like $SrTa_2O_6$ precipitates are also analyzed as well as its interface with the matrix.

Keywords: $SrBi_2Ta_2O_9$; $SrBi_2Ta_{1.6}Nb_{0.4}O_9$; Ferroelectric ceramic; Hot-press sintering; Domain structure

1. Introduction

Ferroelectric ceramics have attracted much attention due to their potential applications in photocatalytic splitting of water into H_2 and O_2 [1], and in electronic devices such as pyroelectric infrared detectors, optical switches, actuators, dynamic random access memories (DRAMS), and non-volatile random access memories (NVRAMS) [2–5]. In particular, $SrBi_2Ta_2O_9$ (SBT), one of the bismuth layered structure compounds, is a promising candidate for ferroelectric random access memories (FRAMS) due to its excellent fatigue resistance after 10^{12} cycles under polarization switching [6]. SBT and $SrBi_2Nb_2O_9$ (SBN) are called Aurivillius phase [7], and have the general formula of $(Bi_2O_2)^{2+}(A_{m-1}B_mO_{3m+1})^{2-}$, where A and B represent ions with suitable valences and ionic radii (such as Bi, Pb, Ba, Sr, Ca and K for the A site and Ti, Nb, Ta, W, Mo, Fe and Cr for the B site, respectively). A pseudo-perovskite layer ($A_{m-1}B_mO_{3m+1}$) is sandwiched between the fluorite type sheets $(Bi_2O_2)^{2+}$, where m and $m-1$ are the numbers of oxygen octahedral and pseudo-perovskite units in one layer, respectively. A lot of attempts to improve properties of SBT and SBN materials by doping (W^{6+}, V^{5+}, Sb^{3+} and Sn^{2+}) have been reported [8–13]. Idemoto et al. [14] investigated the relationship between the average and local crystal structures and found enhancement in ferroelectric properties of Bi_2SiO_5, $Bi_4Si_3O_{12}$, or Bi_2O_3 added $Sr_{1-x}Bi_{2+x}Ta_2O_9$ ($x = 0$, 0.2) produced by a solid-state reaction. There have been a large number of reports on the synthesis and characterization of SBT and SBN powder, thin film and bulk ceramics in the literature recently [15–19]. Polymeric precursor method was used to prepare both $SrBi_2(Ta_{0.5}Nb_{0.5})_2O_9$ (SBTN) thin films [20] and tungsten ion (W^{6+}) substituted SBTN thin films [21]. Textured $SrBi_2Ta_2O_9$ (SBT) ceramics were fabricated *via* template grain growth (TGG) technique using platelet-like SBT single crystal templates [22]. SBT ceramics were mostly synthesized using conventional solid state reaction in which relatively high sintering temperature, usually exceeding 1200 °C, and long sintering time (12–30 h) were required [23–25]. The most commonly used grain orientation technique is the hot-forging method which results in the spontaneous polarization being in the grain-oriented *c*-plane.

A typical microstructure of SBT (T_c = 300 °C) is the 180° ferroelectric domain configuration and this may be the reason for good fatigue properties. While SBT exhibits lower remnant

* Corresponding authors. Tel.: +86 451 8640 2040x8404; fax: +86 451 8641 4291.
E-mail addresses: wangwen@hit.edu.cn (W. Wang), jcrao@hit.edu.cn (J. Rao).

0272-8842/$36.00
doi:10.1016/j.ceramint.2012.01.050

polarization (P_r), higher coercive field (E_c), and higher leakage current than SBN (T_c = 440 °C). Although, partial substitution of Nb for Ta in SBT has been investigated to provide a material with enhanced ferroelectric properties, the microstructure and domain morphologies of SBT ceramics are still unknown. In addition, to our best knowledge, the electric domain structure of the SBT (or SBTN) ceramics has been rarely observed. Herein we report domain structure in SBTN ceramics prepared by hot-press process.

2. Experimental

The SBTN and SBT ceramics were synthesized by hot-press sintering with the starting powders prepared by a new sol–gel method. Since the samples were possibly contaminated by graphite mould during sintering, the disk samples were buried in SBT powder and heat treated for decarbonizing at 1000 °C in air for 1 h.

The relative density was measured by the Archimedes method. The phase structure of samples was examined by X-ray diffraction (XRD) with a scanning speed of 10°/min. The morphology of the samples was determined by a scanning electron microscope (SEM). Samples for TEM observation were prepared by conventional mechanical thinning, followed by Ar ion milling. A JEM ARM 1000 TEM operated at 1000 kV was used for this study. Hysteresis (P–E) loop measurement was performed using a Radiant Technology RT 66A ferroelectric test system.

3. Results and discussion

The as-sintered $SrBi_2Ta1.6Nb_{0.4}O_9$ (SBTN) and un-doped SBT materials had almost equal relative densities of 98.88% and 98.97%, respectively. The crystal structure of as-sintered SBTN is proved by XRD results as shown in Fig. 1 to have a single perovskite phase with layered structure, which is similar to that of SBT. However, the lattice constants exhibit significant difference with a, b and c of 0.5522, 0.5524 and 2.5026 nm,

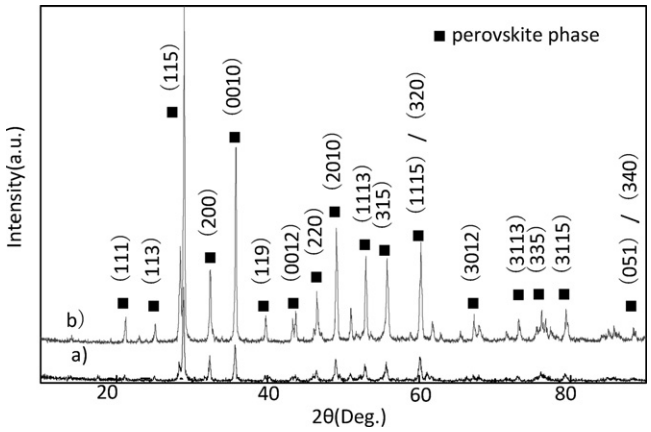

Fig. 1. XRD profiles of decarbonized $SrBi_2(Ta_{1-x}Nb_x)_2O_9$ ceramics: (a) $SrBi_2Ta_{1.6}Nb_{0.4}O_9$; (b)$SrBi_2Ta_2O_9$.

respectively. Obviously, the lattice constants a and b decrease, while c increases, by doping with Nb into the SBT lattice. The substitution of Nb for Ta is responsible for these variations as pentavalent niobium ions (radius of 0.068 nm) are larger than pentavalent tantalum ions (radius of 0.064 nm). Meanwhile the results of calculated intensity of various planes show that the intensity ratio (I_{008}/I_{200}) of (0 0 8) to (2 0 0) is clearly larger than that of the un-doped SBT in which the XRD profile is close to the data in JCPDF 49-0609. The I_{008}/I_{200} values of the $SrBi_2Ta_{1.6}Nb_{0.4}O_9$ and the un-doped SBT are 0.43 and 0.17, respectively. This indicates that there exist some preferred orientations such as {0 0 8} planes formed during the sample preparation.

SBT is a typical member of the family of bismuth-layered perovskite ferroelectric oxides. Its crystal structure belongs to orthogonal system with space group of true ferroelectric $A2_1am$. Ferroelectric domain structures in SBT single crystal materials have been investigated by the theory of space groups [26,27]. Theoretically analysis determined there are five kinds of domain walls in SBT, *i.e.* 90° domain wall, 180° domain wall, antiphase boundaries (APBs), APBs combined with 90°

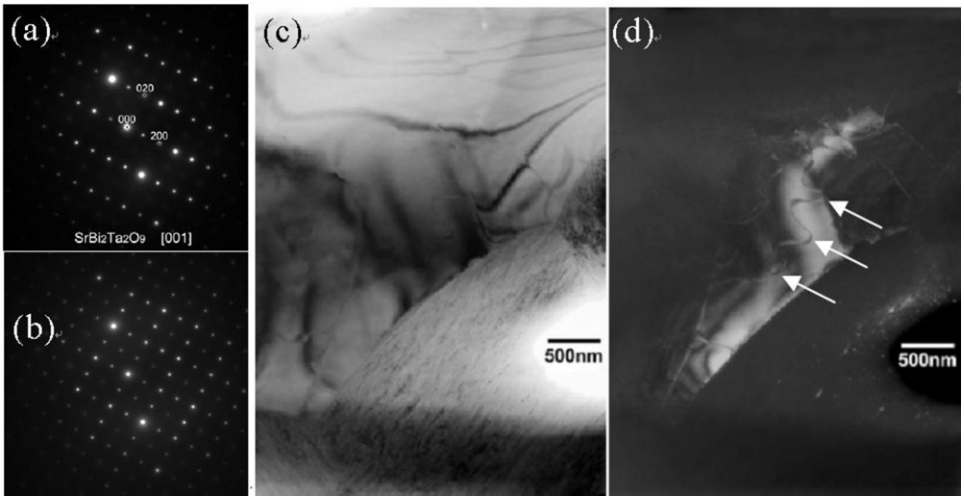

Fig. 2. 90° domain structure in SBT: SAD pattern in [0 0 1] direction of one domain (a), and of two domains oriented by 90° mutually (b) in undoped SBT. Curved domain walls are obvious both in BF (c) and DF (d) of (1 2 0) diffraction spot.

domain wall, and APBs combined with 180° domain wall. The relationships between different ferroelectric domains are just a 90° or 180° rotation around *c* axis. In reciprocal space, the lattice of two domains with 180° rotation overlap each other totally. Therefore, in a dark field image with an (odd 0 0) superlattice diffracted spot from one domain, other domains can also be observed. The boundaries of domains are then identified with a contrast. Fig. 2(a) shows a typical electron diffraction pattern of one domain in [0 0 1] direction, while Fig. 2(b) shows a diffraction pattern from two domains with a rotation of 90° mutually. Fig. 2(c) and (d) shows the domain structures both in bright field and in dark field images of (1 2 0) spot, respectively. With the help of the break of Friedel's law, the 180° domain walls and anti-phase boundaries APBs in Nb-doped SBT ceramics are also observed in the dark field using the (1 2 0) superlattice spot. The curved domain boundaries are obvious in the dark field image as shown by arrows. Other domain boundaries were also observed with (1 0 0), (3 0 0), (5 0 0) spots in [0 0 1] direction of $SrBi_2Ta_2O_9$ phase. Fig. 3 shows both the bright and dark field images of (5 0 0) spot. The boundary between bright and dark domains is a 90° domain wall and that between two bright or two dark domains is a 180° one. More interestingly, however, the traditional 90° domain can be found in the SBT ceramics, which are the evidence of large strains in the lattice. Fig. 4 gives the bright field and dark field morphology of the traditional 90° domain structures. During hot-press sintering of SBT samples, the elastic strain plays a very important role in forming the domain structure. However, it is known that the type of domain wall of SBT is determined by the dipole–dipole interactions and domain wall energies. Therefore, the long-range elastic strain also dictates the domain structure for the SBT. It reveals that the domain structure of the SBT is similar to typical ferroelectrics.

The crystal structures of the impurities were also analyzed in TEM. There are typical rod-like precipitates both in up-doped

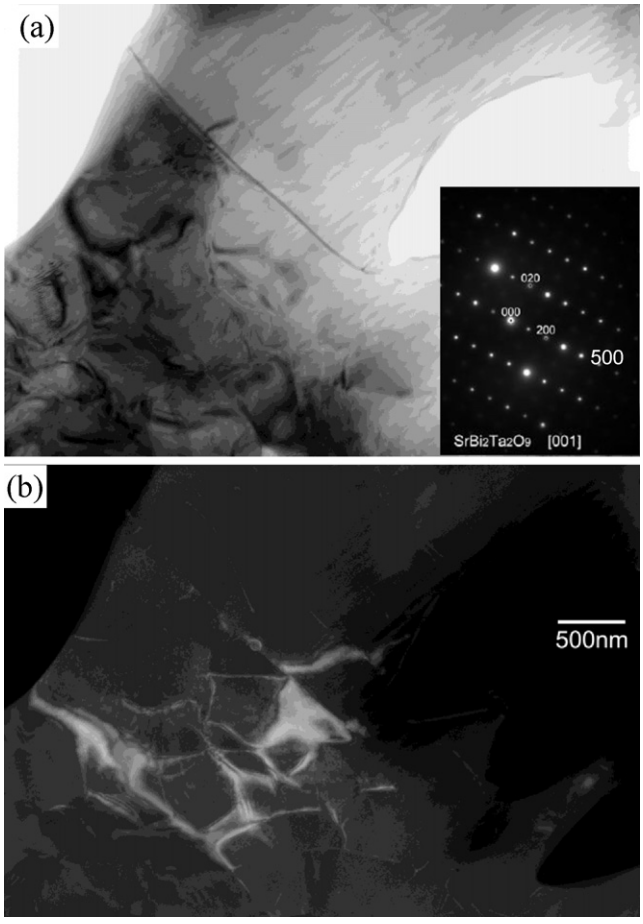

Fig. 3. 180° domain structure in SBT: Domain structure in BF (a) and DF (b) images observed with (5 0 0) spot in the SAD pattern of undoped SBT (c). Bended 180° domain wall is obvious.

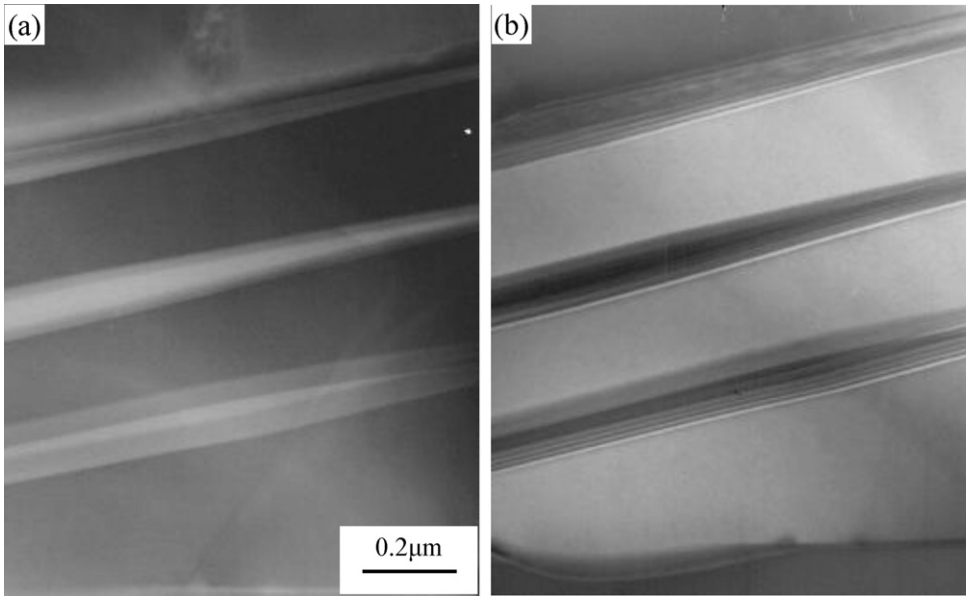

Fig. 4. Traditional 90° domain walls in hot-press sintered $SrBi_2Ta_2O_9$: (a) BF; (b) DF.

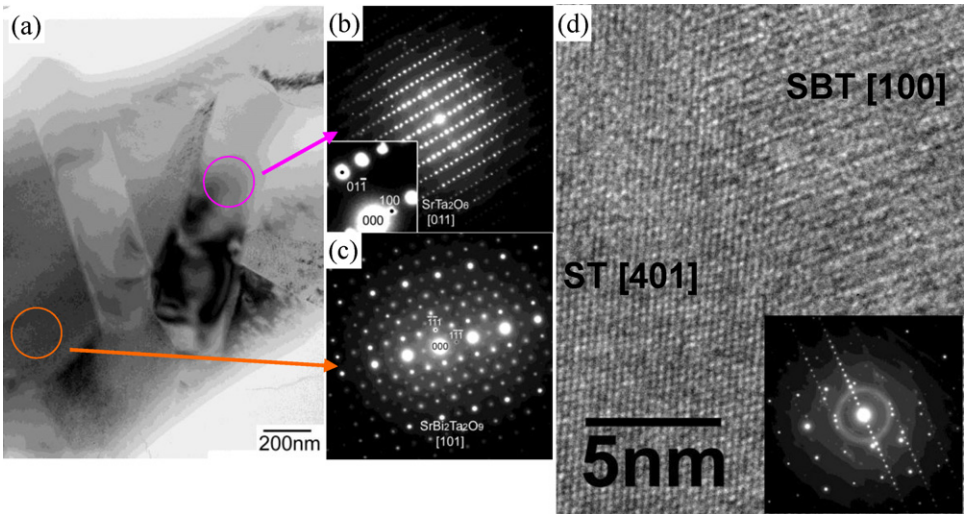

Fig. 5. Rod-like structures in Nb doped SBT matrix. (a) Low magnification image of rod-like structures and SBT matrix; (b) SAD pattern from one rod-like structure; (c) SAD pattern from SBT matrix; (d) high-resolution images of the interface between another rod-like phase and SBT matrix with diffraction pattern inserted.

and Nb doped SBTs. Fig. 5(a) shows the BF morphology of the rod-likes structures. Fig. 5(b) and (c) are the SAD patterns from one rod-like grain and from SBT matrix, respectively. An enlarged area near direct beam was inserted in Fig. 5(b) for clarity. The rod-like phase is identified as $SrTa_2O_6$ phase based on the results both of SAD and Energy-Dispersive X-ray Spectroscopy (EDS) analysis. The content of Bi around the impurities is deficient, and the mole ratio of Sr to Ta is about 1:3. Small amounts of Nb can also be detected by EDS. This is attributed to evaporation of a small amount of Bi_2O_3 (melting point about 820 °C) during sintering process. HRTEM micrograph in Fig. 5(d) shows the interface clearly between $SrTa_2O_6$ (ST) precipitate and SBT matrix. It is obvious that the interface is clear and straight without any other phases. The contrast near interface in SBT side indicates the small strain due to the low lattice mismatch between ST precipitate and SBT matrix. The combined SAD pattern is inserted.

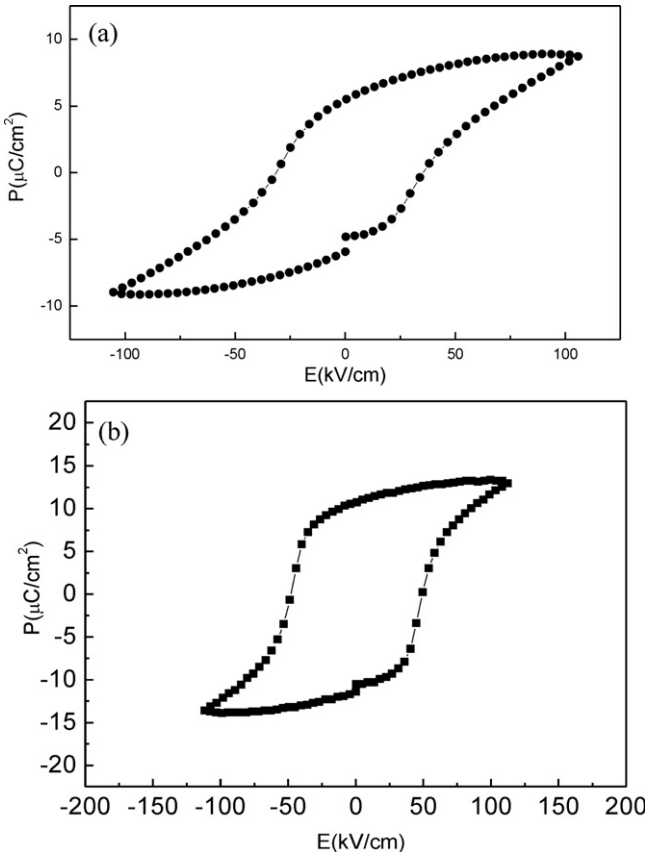

Fig. 6. Hysteresis loop of $SrBi_2Ta_2O_9$ (a) and $SrBi_2Ta_{1.6}Nb_{0.4}O_9$ (b) ceramics.

Fig. 6 shows the hysteresis loop of SBT and SBTN ceramics. *P–E* hysteresis loops show P_r increases from 5.5 μC/cm^2 to 12 μC/cm^2, and E_c increases from 35 kV/cm to 50 kV/cm. Atomic displacement of the ions in the $(Ta,Nb)O_6$ octahedron significantly increases as the amount of Nb doping increasing, which leads to more structural distortion of the perovskite-type unit. The contribution of the perovskite-type unit to total ferroelectric polarization increases with the amount of Nb doping increasing.

4. Conclusion

$SrBi_2(Ta_{1-x}Nb_x)_2O_9$ ($x = 0, 0.2$) ferroelectric ceramics were synthesized with a reactive hot-press sintering process. The as-sintered SBTN materials had a maximum relative density of 98.88%. The lattice constants *a* and *b* decrease and *c* increases after Nb doping into SBT. The TEM and HRTEM observation results show (0 0 8) preferred orientations of grains, which matches well with the XRD results. The 90° domain walls are identified by a 90° rotation relationship of the electron diffraction pattern along the [0 0 1] zone axis. Irregular shaped and highly curved 180° domain wall were also observed in SBTN ceramics. The traditional 90° domain walls are also found in the hot-press sintered SBT ceramics, which are the evidence of large strains in the lattice. Rod-like $SrTa_2O_6$ precipitates are also analyzed as well as its interface with the matrix.

Acknowledgements

The authors would like to thank the financial support from National Natural Science Foundation of China with the Project Nos. 50872024 and 51021002, NSFC-RFBR Joint Project No. 51011120099, the Fundamental Research Funds for the Central Universities (Grant No. HIT.NSRIF.2009031), and Harbin Science Foundation No. 2011RFLXG005.

References

[1] Y. Li, G. Chen, H. Zhang, Z. Li, J. Sun, Electronic structure and photocatalytic properties of $ABi_2Ta_2O_9$ (A = Ca, Sr, Ba), J. Solid State Chem. 181 (2008) 2653–2659.

[2] J.Z. Liu, K.W. Kwok, H.L.W. Chan, C.L. Choy, Dielectric properties and relaxation of $SrBi_2(Nb_{0.25}Ta_{0.75})_2O_9$ ceramic at RF frequency, J. Eur. Ceram. Soc. 24 (2004) 1769–1773.

[3] C. Fujioka, R. Aoyagi, H. Takeda, S. Okamura, T. Shiosaki, Effect of non-stoichiometry on ferroelectricity and piezoelectricity in strontium bismuth tantalate ceramics, J. Eur. Ceram. Soc. 25 (2005) 2723–2726.

[4] Y. Wu, G. Cao, Ferroelectric and dielectric properties of strontium bismuth niobate vanadates, J. Mater. Res. 15 (2000) 1583–1590.

[5] Y. Wu, M. Forbess, S. Seraji, S. Limmer, T. Chou, G. Cao, Influence of oxygen annealing on the dielectric properties of $SrBi_2(V_{0.1}Nb_{0.9})_2O_9$ ceramics, J. Phys. D: Appl. Phys. 34 (2001) 2665–2669.

[6] C. Araujo, J.D. Cuchlaro, L.D. McMillan, M.C. Scott, J.F. Scott, Fatigue-free ferroelectric capacitors with platinum electrodes, Nature 374 (1995) 627–629.

[7] B. Aurivillius, P.H. Fang, Ferroelectricity in the compound $Ba_2Bi_4Ti_5O_{18}$, Phys. Rev. 126 (1962) 893–896.

[8] I. Coondooa, A.K. Jha, S.K. Agarwal, Enhancement of dielectric characteristics in donor doped Aurivillius $SrBi_2Ta_2O_9$ ferroelectric ceramics, J. Eur. Ceram. Soc. 27 (2007) 253–260.

[9] I. Coondoo, S.K. Agarwal, A.K. Jha, Ferroelectric and piezoelectric properties of tungsten substituted $SrBi_2Ta_2O_9$ ferroelectric ceramics, Mater. Res. Bull. 44 (2009) 1288–1292.

[10] D. Kajewski, Z. Ujma, K. Szot, M. Pawełczyk, Dielectric properties and phase transition in $SrBi_2Nb_2O_9$–$SrBi_2Ta_2O_9$ solid solution, Ceram. Int. 35 (2009) 2351–2355.

[11] D. Kajewski, Z. Ujma, Electrical properties of $SrBi_2(Nb_{0.5}Ta_{0.5})_2O_9$ ceramics, J. Phys. Chem. Solids 71 (2010) 24–29.

[12] R. Sridaranea, S. Subramanianb, N. Jananic, R. Muruganc, Investigation on microstructure, dielectric and impedance properties of $Sr_{1-x}Bi_{2+(2/3)x}(V_xTa_{1-x})_2O_9$ [x = 0, 0.1 and 0.2] ceramics, J. Alloy Compd. 492 (2010) 642–648.

[13] P. Millan, A. Ramirez, A. Castro, Substitution of smaller Sb^{3+} and Sn^{2+} cations for Bi^{3+} in Aurivillius-like phases, J. Mater. Sci. Lett. 14 (1995) 1657–1660.

[14] Y. Idemoto, S. Taniyama, S. Iikubo, S. Shamoto, J.W. Richardson, Relationship between average and local crystal structure and the ferroelectric properties of a Sr–Bi–Ta–Si–O ferroelectric material, J. Phys. Chem. Solids 70 (2009) 1156–1165.

[15] S. Ezhilvalavan, V. Samper, T.W. Seng, X. Junmin, J. Wang, Ferroelectric properties and leakage current mechanisms in $SrBi_2(V_{0.1}Nb_{0.9})_2O_9$ (SBVN) thin films, Ceram. Int. 30 (2004) 1505–1508.

[16] J. Lettieri, M.A. Zurbuchen, Y. Jia, D.G. Schlom, S.K. Streiffer, M.E. Hawley, Epitaxial growth of non-c-oriented $SrBi_2Nb_2O_9$ on (1 1 1) $SrTiO_3$, Appl. Phys. Lett. 76 (2000) 2937–2939.

[17] K. Babooram, Z.G. Ye, New soft chemical routes to ferroelectric $SrBi_2Ta_2O_9$, Chem. Mater. 18 (2006) 532–540.

[18] A.B. Panda, A. Tarafdar, A. Pathak, P. Pramanik, Chemical synthesis and characterization of nanocrystalline $ABi_2Ta_2O_9$ (A = Sr, Ba and Ca) powders, Ceram. Int. 30 (2004) 715–720.

[19] N.L. Junior, A.Z. Simoes, A.A. Cavalheiro, S.M. Zanetti, E. Longo, J.A. Varela, Structural and microstructural characterization of $SrBi_2(Ta_{0.5}Nb_{0.48}W_{0.02})_2O_9$ powders, J. Alloy Compd. 454 (2008) 61–65.

[20] N.L. Junior, A.Z. Simoes, R.F. Pianno, S.M. Zanetti, E. Longo, J.A. Varela, Structural and electrical properties of $SrBi_2(Ta_{0.5}Nb_{0.5})_2O_9$ thin films, J. Alloy Compd. 458 (2008) 500–503.

[21] N.L. Junior, A.Z. Simoes, L.S. Cavalcante, F. Moura, E. Longo, J.A. Varela, $SrBi_2(Ta_{0.5}Nb_{0.5})_2O_9$:W thin films obtained by chemical solution deposition: morphological and ferroelectric characteristics, J. Alloy Compd. 461 (2008) 326–330.

[22] H. Amorin, A.L. Kholkin, M.E. Costa, Templated grain growth of $SrBi_2Ta_2O_9$ ceramics: mechanism of texture development, Mater. Res. Bull. 43 (2008) 1412–1419.

[23] Y. Wu, C. Nguyen, S. Seraji, M. Forbess, S.J. Limmer, T. Chou, G. Cao, Processing and properties of strontium bismuth vanadium niobate ferroelectric ceramics, J. Am. Ceram. Soc. 84 (2001) 2882–2888.

[24] S. Inai, Y. Hiruma, M. Suzuki, H. Nagata, T. Takenaka, Temperature dependences of piezoelectric properties of vanadium substituted $SrBi_2Nb_2O_9$ ceramics with grain orientation, Ceram. Int. 34 (2008) 741–744.

[25] B.J. Kalaiselvi, R. Sridarane, R. Murugan, Dielectric properties of $Sr_{1-x}Bi_{2+(2/3)x}(V_xNb_{1-x})_2O_9$ [x = 0.1 and 0.2] ceramics, Ceram. Int. 32 (2006) 467–470.

[26] X.H. Zhu, J.M. Zhu, S.H. Zhou, Q. Li, Z.G. Liu, N.B. Ming, Microstructures of SBT materials investigated by transmission electron microscopy, J. Chin. Electron Microsc. Soc. 21 (2002) 287–292.

[27] A.D. Rae, J.G. Thompson, R.L. Withers, Structure refinement of commensurately modulated bismuth strontium tantalate $Bi_2SrTa_2O_9$, Acta Crystallogr. B 48 (1992) 418–428.